Conversion of the arterial input function using accelerated dual-contrast EPIK: a multi-modality MR-PET study

Liliana Lourenco Caldeira [1], Seong Dae Yun[1], Nuno André da Silva[1], Christian Filss[1], and N. Jon Shah[1,2]

[1]*Institute of Neuroscience and Medicine (4), Forschungszentrum Juelich, Jülich, Germany,* [2]*RWTH Aachen University, Faculty of Medicine, Department of Neurology, JARA, Aachen, Germany*

Target Audience: Individuals interested in the arterial input function and parametric imaging.

Purpose: The arterial input function (AIF) is essential for quantification in MRI and PET. The AIF is a function that describes the arrival of contrast agent to the tissue of interest. The gold standard for AIF estimation is arterial cannulation, which is an invasive and laborious procedure. Alternatively, an image-derived AIF can be estimated using MRI and/or PET images. For an appropriate estimation of the AIF, a reasonable temporal resolution of dynamic image series is necessary (<2s). In PET, the minimum frame length is usually 5s and therefore these images are rather noisy. In MRI, higher temporal resolution can be achieved for AIF estimation. For accurate AIF localization (e.g. carotid artery), it is necessary to have a reasonable spatial resolution ($2\times2\times5mm^3$). For this purpose, the present work uses the dual-contrast accelerated EPI with keyhole (EPIK)[1,2] scheme for the DSC-MRI acquisition, which has been validated to have a sufficient time and spatial resolution for an adequate AIF estimation[3,4]. The proposed method is demonstrated with 8 patient measurements where Gd-DTPA contrast was injected while simultaneously acquiring [18F]-FET data.

Methods: A Siemens (Erlangen, Germany) hybrid 3T MR-BrainPET scanner with an 8-channel phased array coil from the manufacturer was used. A simultaneous brain MR-PET acquisition was performed on a group of 8 patients (see Table 1). The PET tracer [18F]-FET was injected manually (3MBq/Kg of body weight) while the patients were inside the scanner and thus the AIF can be estimated. PET data were acquired in list-mode format, which can then be sorted into appropriate frames. PET images were reconstructed with the following 23 frames using standard reconstruction protocol: 8x5s, 2x10s, 2x15s, 1x30s; 1x60s; 1x120s; 5x300s; 3x600s. All PET corrections were taken into account: normalisation, randoms, scatter and attenuation. PET images have 256x256x153 voxels and 1.25mm isotropic voxel. For AIF extraction, the PET data were filtered with a $2.5mm^3$ Gaussian Filter. Gd-DTPA was administered to the patient with a power injector (Injektron 82 MRT Medtron AG) while the EPIK sequence was running (0.1mmol/Kg of body weight). The MR data were acquired using two-fold accelerated dual-contrast (DC) EPIK. The acquisition scheme was realised by first accelerating the original EPIK scheme with a parallel MRI acceleration factor of two, resulting in two-fold accelerated EPIK. Next, two-fold EPIK was repeated twice per TR to acquire dual contrasts defined by TE_1 and TE_2 (two-fold DC-EPIK); the dual contrasts may help to provide additional information on tumour biology in a clinical setting by providing parametric images[5]. The MR data were acquired using following parameters: FOV=240×240 mm², matrix size=128×128, $TR/TE_1/TE_2$=1000/13/33 ms, slice thickness=5 mm with 24 slices and 50 temporal volumes. The proposed acquisition provides a unique framework to study AIF estimation methods using PET and MRI images for human studies. It has been shown in the literature that the AIFs obtained with PET and MR data have similar features and can be converted into one another[6]. Moreover, there are several possibilities to model the AIF, but we used a gamma-function fitting as this is the most common fitting for MRI signals and it is also accepted for PET signals: $S(t)=A.(t-BAT)^B.\exp(-(t-BAT)/C)$, where A is amplitude, BAT is the bolus arrival time and B and C are the shape parameters. Using the gamma functions from both modalities, a relationship between the MRI and PET AIFs can be established. A post-contrast MPRAGE was also acquired for all patients allowing definition of region-of-interest for the AIF (carotid arteries). Carotid segmentation was performed with a semi-automatic method in PMOD (PMOD Technologies Ltd., Switzerland).

Table 1 – Group of 8 patients with simultaneous MR-PET acquisition.

#	Tumor Type	WHO Grade
1	Oligodendroglioma	III
2	Oligodendroglioma	II
3	Anaplastic Astrocytoma	III
4	Suspicious of Glioma	-
5	Suspicious of Glioma	-
6	Glioblastoma	IV
7	Anaplastic Oligoastrocytoma	III
8	Glioblastoma	IV

Results: First, AIFs from both EPIK and [18F]-FET were extracted from the images (only 10 voxels from each modality were used). Then, gamma function fitting was performed using Matlab (*nlinfit*). In Fig.1(a), these curves are depicted. When using the gamma function only the first bolus passage is modelled, although the second passage of the bolus can be seen in both modalities (Fig. 1(a)). Then, relationships between the parameters of both fitted gamma functions (MRI and PET) were evaluated. The gamma-function shape parameters (B and C) and the amplitude (A) have a strong linear relationship. Resuming, the estimated linear relationships are: $B_{PET}=0.83B_{MRI}+1.38$, $R^2=0.86$; $C_{PET}=1.059C_{MRI}-0.05$, $R^2=0.98$; $A_{PET}=0.45A_{MRI}+0.0015$, $R^2=0.92$. The BAT is different between the two acquisitions, probably due to the fact that PET tracer injection is performed manually, while the MRI contrast agent injection is performed automatically. Using the relationships obtained, a conversion between the MRI and PET AIF can be carried out. In Fig. 1(a), the conversion curve can be seen and it is rather similar to the original PET curve. Fig. 1(b) shows the images from this patient data. In these images, it can be seen that the EPIK images show a decrease of signal after contrast agent injection as expected. Furthermore, MPRAGE images clearly show the carotid arteries which were used to define ROIs for the AIF. The [18F]-FET images are rather noisy, as expected, even after the application of Gaussian filter (Fig. 1(b)).

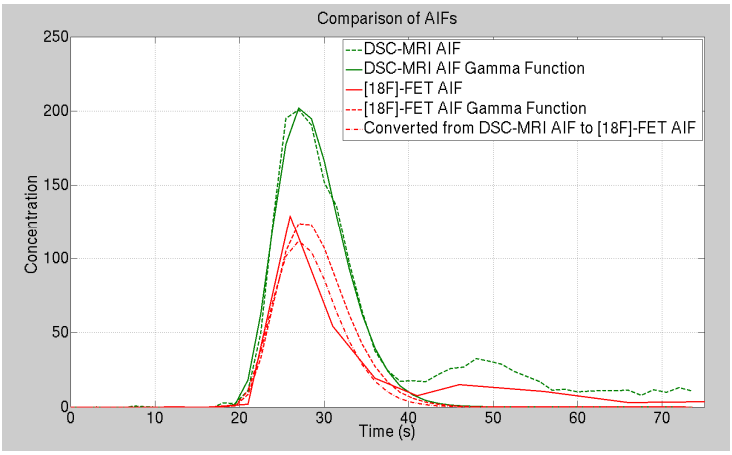

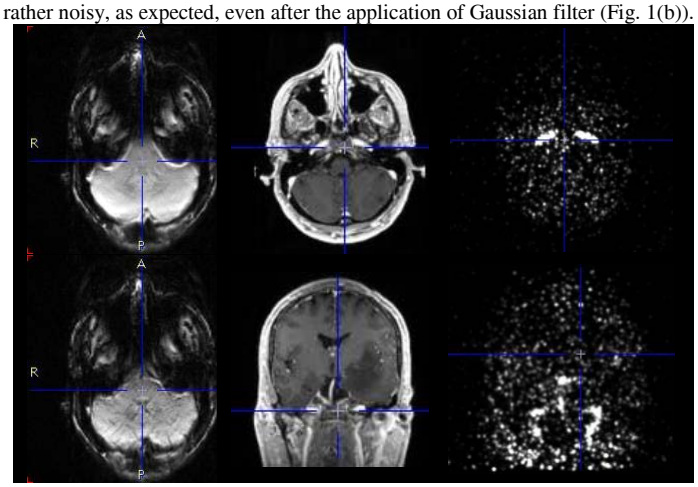

Figure 1 - (a) Graph with AIFs obtained with the two modalities, corresponding gamma-fitting functions and the AIF converted from DSC-MRI to [18F]-FET. (b) From left right, top to bottom: transverse EPI image before contrast agent, transverse MPRAGE, transverse [18F]-FET (Frame 4), transverse EPIK image after contrast agent, coronal MPRAGE after contrast agent and coronal [18F]-FET (Frame 4).

Discussion: The estimated AIF from EPIK data had a similar shape to that from the [18F]-FET data. Relationships for conversion of parameters were found. However, one should mention that both DC-EPIK and [18F]-FET have not been corrected for partial volume effects, delay and dispersion (an additional invasive procedure is required) and therefore, the shape of curves might be slightly affected. Furthermore, two-fold accelerated DC-EPIK allows the acquisition of dual-contrast information in a similar acquisition time of a comparable two-fold accelerated EPI and thus the accelerated DC-EPIK method is of great interest for characterisation of the AIF.

Conclusion: In this work we have demonstrated the simultaneous acquisition of a dynamic PET and MRI series with two-fold accelerated DC-EPIK. This is the first time that simultaneous DSC-MRI and [18F]-FET AIFs are presented for human patients. This work has the potential to enable image-derived AIF in a clinical context using hybrid MR-PET. The obtained dynamic MRI series allowed estimation of the AIF with a high temporal resolution of 1.5s and it had a similar shape to the one from the [18F]-FET data (5s temporal resolution). In the future, we will extend this study to more patients and work on an automatic carotid segmentation method.

References:1. Zaitsev M, Zilles K, Shah NJ. Magn Reson Med. 2001 45(1):109-17. 2.Yun S, Reske M, Vahedipour K, et al. Neuroimage 2013;73;135-143. 3. Zaitsev M, Arcy JD, Collins DJ, et al. Phys Med Biol 2005;50:4491-4505. 4. Caldeira L, Yun S, da Silva N, Filss C, Shah NJ. Proceeding ISMRM 2013. 5. Barbier EL, Lammale L, Décorps M. Journal of Magnetic Resonance Imaging 2001;13(4);496-520. 6. Poulin E, Croteau E, Blanchette M, et al. Magn Reson Med. 2013;69(3);781-792.